Journal of Physics: Conference Series

PAPER • OPEN ACCESS

A Fully Geometric Approach for Inverse Kinematics of a Six-Degree-of-Freedom Robot Arm

A Fully Geometric Approach for Inverse Kinematics of a Six-Degree-of-Freedom Robot Arm

Hongsheng Zhang[1a*], Qianjin Xia[1b], Jinchao Sun[2c], Qingjuan Zhao[2d]

[1] Department of Large Aircraft, Ordos Institute of Technology, Ordos 017000, Inner Mongolia, China

[2] College of Mechanical and Control Engineering, Guilin University of Technology, Guilin541004, China

[a*]zhs293@gmail.com, [b]xqj10@tsinghua.org.cn, [c]18052399135@163.com, [d]lanxi0211@163.com

Abstract—This paper presents an analytical solution to inverse kinematics problem of a 6-DOF robot arm based on geometric method. The solution only utilizes relations between vectors in frames attached in the robot arm. Experiments with the solution are conducted to test the approach and results show that the correctness and accuracy of the solution are verified.

1. Introduction

Articulated robot arms are used in more and more industries because of their flexibility and ability to handle different tasks to avoid injuries and health harm. In robotics, inverse kinematics is solving the problem of finding required joint angles of robot arm to place the end effector to a target. Inverse kinematics plays a key role since the approach determines precision and calculation time. The solution strategies are generally split into two classes: numerical solutions and analytical (or closed-form) solutions which include algebraic and geometric methods [1].

Numerical methods perform iterative calculation mainly based on Newton-Raphson or Gauss-Newton method [2]. One major drawback of numerical methods that it is more time consuming when executing real time tasks. However, powerful chips with increasing computing ability become a remedy. Kalajahi and Mahboukkhah [3] compared numerical and analytical solutions of direct kinematics in a four-degree of freedom (4-DOF) parallel robot and found that numerical solution is even quicker with acceptable accuracy. There are some advantages of numerical methods, such as avoiding deadlock caused by joint limits and providing solutions for the robots which don't have analytical solutions [4, 5]. Analytical solutions are available only for special cases. Hemami and Labonville [6] presented analytical solutions for kinds of industrial robot arms. For a general 6-DOF robot arm, the traditional approach is solving non-linear equations through algebraic method [7-9]. Khatamian [10] presented an analytical approach which combines geometric method and algebraic method for a 6-DOF robot arm. Recently, redundant robot arms have been studied a lot and new methods such as artificial intelligence have been applied to kinematics of robot arm [11-15].

This study aims to present a fully geometric approach for solving inverse kinematics problem of a 6-DOF robot arm. The robot arm structure is used by many industrial robots. The rest of this paper describes details of the derivation and experiment.

Table 1 D-H parameters of the 6-DOF robot arm

i	α_{i-1}	a_{i-1}	d_{i-1}	Θ_i
1	0	0	d1	Θ_1
2	-0.5π	0	0	-0.5π+Θ_2
3	0	a_2	0	0.5π+Θ_3
4	0.5π	0	d_4	Θ_4
5	-0.5π	0	0	Θ_5
6	-0.5π	0	d_6	Θ_6

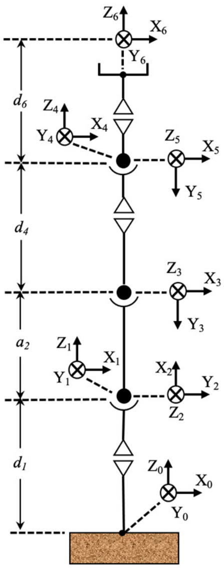

Fig.1 A symbolic structure of robot arm

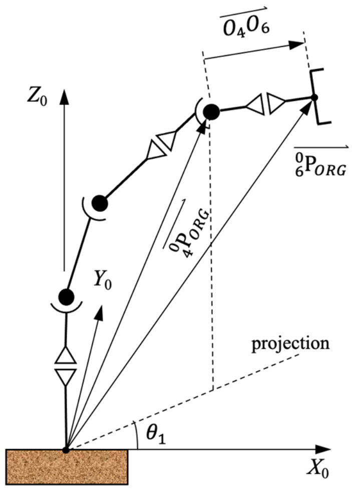

Fig.2 Joint angle calculation for joint 1

2. Robot arm description

To derive fully geometric solutions, this study adopts a general six-degree-of-freedom robot arm, which has six revolute joints and has three neighboring joint axes intersecting at a point. A symbolic structure of the robot arm is shown in Fig.1. Many industrial robot arms have the same structure as shown in Fig.1. By taking the Denavit-Hartenberg (D-H) convention, a frame is attached to each link, and the base frame is fixed on the base. The D-H parameters of the robot arm are listed in Table 1.

A homogeneous transformation matrix ${}^0_6T$ is constructed to state the orientation and position of end effector of the robot arm relative to the base and it is as follows:

$$ {}^0_6T = \begin{bmatrix} {}^0_6R & {}^0_6P_{ORG} \\ 0 & 1 \end{bmatrix} = \begin{bmatrix} {}^0_6R_{11} & {}^0_6R_{12} & {}^0_6R_{13} & {}^0_6P_{ORGx} \\ {}^0_6R_{21} & {}^0_6R_{22} & {}^0_6R_{23} & {}^0_6P_{ORGy} \\ {}^0_6R_{31} & {}^0_6R_{32} & {}^0_6R_{33} & {}^0_6P_{ORGz} \\ 0 & 0 & 0 & 1 \end{bmatrix} \tag{1} $$

where ${}^0_6R$ a rotation matrix which describes the sixth frame relative to the base frame and ${}^0_6P_{ORG}$ is a position vector of the end effector in the base frame.

3. Inverse kinematic

The geometric approach to find required joint angles employs vectors which describe the robot state in the space. This section presents details of solving each joint angle.

3.1. Joint 1

As shown in Fig.1, the first four links are all the time on a same plane which is perpendicular to the horizontal plane. Therefore, the first joint angle can be found by taking projection of the plane that the first four links fallen in. As shown in Fig.2, there exist such relations between vectors as follows

$$\overrightarrow{{}_4^0P_{ORG}} = \overrightarrow{{}_6^0P_{ORG}} - \overrightarrow{O_4O_6} \tag{2}$$

where $\overrightarrow{{}_4^0P_{ORG}}$ is the vector originating from the base frame origin to the origin of coordinate $X_4Y_4Z_4$ and $\overrightarrow{O_4O_6}$ is the vector originating from the origin of coordinate $X_4Y_4Z_4$ to the origin of coordinate $X_6Y_6Z_6$. The vector $\overrightarrow{O_4O_6}$ is aligned with the Z axis of coordinate system $X_6Y_6Z_6$, so it can be calculated as follows

$$\overrightarrow{O_4O_6} = d_6 * \overrightarrow{{}_6^0Z_6} = d_6 * \begin{bmatrix} {}_6^0R_{13} \\ {}_6^0R_{23} \\ {}_6^0R_{33} \end{bmatrix} \tag{3}$$

where $\overrightarrow{{}_6^0Z_6}$ is z-axis unit vector of the coordinate system $X_6Y_6Z_6$ in the base frame.

Then equation (2) becomes

$$\overrightarrow{{}_4^0P_{ORG}} = \begin{bmatrix} {}_4^0P_{ORGx} \\ {}_4^0P_{ORGy} \\ {}_4^0P_{ORGz} \end{bmatrix} = \begin{bmatrix} {}_6^0P_{ORGx} - {}_6^0R_{13}d_6 \\ {}_6^0P_{ORGy} - {}_6^0R_{23}d_6 \\ {}_6^0P_{ORGz} - {}_6^0R_{33}d_6 \end{bmatrix} \tag{4}$$

The first joint angle (two solutions) can be found through the vector $\overrightarrow{{}_4^0P_{ORG}}$

$$\theta_1 = \begin{cases} Atan2({}_6^0P_{yORG} - {}_6^0R_{23}d6, {}_6^0P_{xORG} - {}_6^0R_{13}d6) \\ Atan2\left({}_6^0P_{yORG} - {}_6^0R_{23}d6, {}_6^0P_{xORG} - {}_6^0R_{13}d6\right) - \pi \end{cases} \tag{5}$$

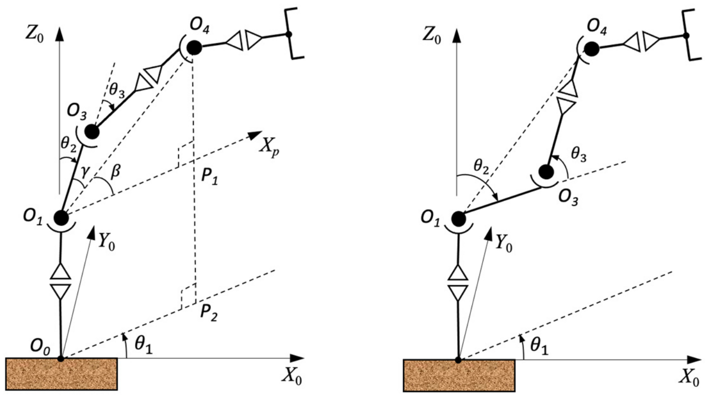

(a) One solution (b) Another solution

Fig.3 Joint angle calculation for joint 3

3.2. Joint 3

According to the illustration in Fig.3, the joint angle of joint 3 can be calculated as long as the edge length of triangle $\Delta O_1O_3O_4$ is known. Since the vector $\overrightarrow{{}_4^0P_{ORG}}$ is already known, the length of $|O_1P_1|$ and $|O_4P_1|$ is easy to calculate. The length of $|O_1O_4|$ is calculated as follows

$$|O_1O_4| = \sqrt{({}_4^0P_{ORGz} - d_1)^2 + {}_4^0P_{ORGx}^2 + {}_4^0P_{ORGy}^2} \tag{6}$$

Using the law of cosines, the joint angle of joint 3 (two solutions) can be found:

$$\theta_3 = \begin{cases} Acos(-\frac{a_2^2+d_4^2-|O_1O_4|^2}{2a_2d_4}) \\ -Acos(-\frac{a_2^2+d_4^2-|O_1O_4|^2}{2a_2d_4}) \end{cases} \tag{7}$$

3.3. Joint 2

As shown in Fig.4, on the plane $O_1O_3O_4$, add a coordinate system $X_pO_1Z_0$ whose x-axis direction in the base frame can be written as

$$\overrightarrow{x_p} = \begin{bmatrix} cos\theta_1 \\ sin\theta_1 \\ 0 \end{bmatrix} \tag{8}$$

The vector $\overrightarrow{O_1O_4}$ in the base frame can be calculated by vector deduction

$$\overrightarrow{O_1O_4} = \overrightarrow{O_0O_4} - \overrightarrow{O_0O_1} = \overrightarrow{{}_4^0P_{ORG}} - \overrightarrow{O_0O_1} = \begin{bmatrix} {}_4^0P_{ORGx} \\ {}_4^0P_{ORGy} \\ {}_4^0P_{ORGz} - d_1 \end{bmatrix} \tag{9}$$

Then the x-coordinate of point O_4 in the coordinate system $X_pO_1Z_0$ is calculated by vector product

$$x_{O_4} = \overrightarrow{O_1O_4} \cdot \overrightarrow{x_p} = {}_4^0P_{ORGx}cos\theta_1 + {}_4^0P_{ORGy}sin\theta_1 \tag{10}$$

So, the coordinates of point O_4 in the coordinate system $X_pO_1Z_0$ are $(x_{O_4}, {}_4^0P_{ORGz} - d_1)$. The angle between vector $\overrightarrow{O_1O_4}$ and the horizontal plane can be calculated as follows

$$\beta = Atan2({}_4^0P_{ORGz} - d_1, {}_4^0P_{ORGx}cos\theta_1 + {}_4^0P_{ORGy}sin\theta_1) \tag{11}$$

The angle γ can be calculated by the law of cosines

$$\gamma = Acos(\frac{a_2^2+|O_1O_4|^2-d_4^2}{2a_2|O_1O_4|}) \tag{12}$$

It's seen from Fig.3 that the joint angle of joint 2 depends on the selection of the joint angle of joint 3. At last, the joint angle of joint 2 can be calculated with a unified form as follows

$$\theta_2 = \frac{\pi}{2} - \beta - sign(\theta_3)\gamma \tag{13}$$

where $sign()$ is a sign function.

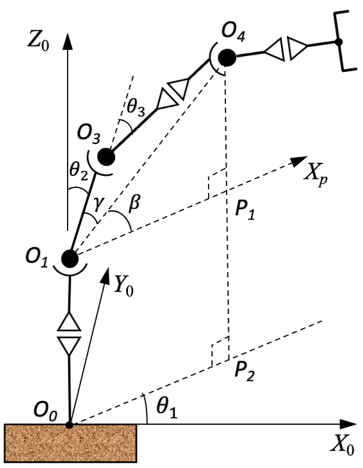

Fig.4 Joint angle calculation of joint 2

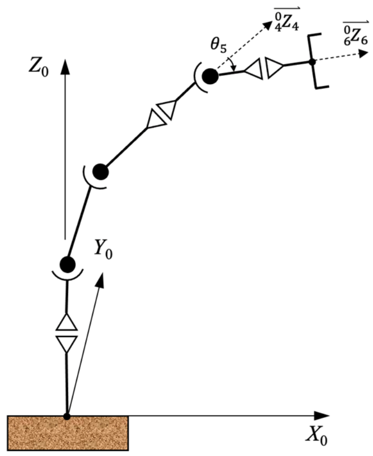

Fig.5 Joint angle calculation of joint 5

3.4. Joint 5

As shown in Fig. 5, no matter what value the joint angle of joint 4 is, the z-axis unit vector of frame 4 in the base frame doesn't change. Now given that the first three joint angles have been found, as long as letting the joint angle of joint 4 be zero, the z-axis unit vector of frame 4 can be achieved through the transformation matrix

$$ {}_4^0T\Big|_{\theta_4=0} = \begin{bmatrix} {}_4^0R'_{11} & {}_4^0R'_{12} & {}_4^0R'_{13} & {}_4^0P_{ORGx} \\ {}_4^0R'_{21} & {}_4^0R'_{22} & {}_4^0R'_{23} & {}_4^0P_{ORGy} \\ {}_4^0R'_{31} & {}_4^0R'_{32} & {}_4^0R'_{33} & {}_4^0P_{ORGz} \\ 0 & 0 & 0 & 1 \end{bmatrix} \tag{14} $$

By the definition of transformation matrix, the *z*-axis unit vector of frame 4 is

$$ \overrightarrow{{}_4^0Z_4} = \begin{bmatrix} {}_4^0R'_{13} \\ {}_4^0R'_{23} \\ {}_4^0R'_{33} \end{bmatrix} \tag{15} $$

Thus, the joint angle of joint 5 is calculated by dot product of $\overrightarrow{{}_6^0Z_6}$ and $\overrightarrow{{}_4^0Z_4}$

$$ \theta_5 = \pm Acos(\overrightarrow{{}_6^0Z_6} \cdot \overrightarrow{{}_4^0Z_4}) \tag{16} $$

3.5. Joint 4

It can be seen from Fig.1 that the *z*-axis unit vector of frame 5 is all the same with the *y*-axis unit vector of frame 4, and the latter vector is always on the X_4Y_4 plane. The joint angle of joint 4 is equal to the angle from the *z*-axis of frame 5 to the *y*-axis of frame 4 when $\theta_4 = 0$ about *z*-axis of frame 4. Thus, as long as the *z*-axis unit vector of frame 5 is determined, the goal can be achieved. It can be observed that cross product of vectors is feasible. In the base frame, the *z*-axis unit vector of frame 5 can be determined by

$$ \overrightarrow{{}_5^0Z_5} = sign(\theta_5)\overrightarrow{{}_4^0Z_4} \otimes \overrightarrow{{}_6^0Z_6} \tag{17} $$

The *x*-axis vector and *y*-axis vector of frame 4 in the base frame can be found in equation (14)

$$ \overrightarrow{{}_4^0X_4}\Big|_{\theta_4=0} = \begin{bmatrix} {}_4^0R'_{11} \\ {}_4^0R'_{21} \\ {}_4^0R'_{31} \end{bmatrix}, \ \overrightarrow{{}_4^0Y_4}\Big|_{\theta_4=0} = \begin{bmatrix} {}_4^0R'_{12} \\ {}_4^0R'_{22} \\ {}_4^0R'_{32} \end{bmatrix} \tag{18} $$

Then we can find the joint angle of joint 4 as shown in Fig.6

$$ \theta_4 = Atan2\left(\overrightarrow{{}_5^0Z_5} \cdot \overrightarrow{{}_4^0Y_4}\Big|_{\theta_4=0}, \overrightarrow{{}_5^0Z_5} \cdot \overrightarrow{{}_4^0X_4}\Big|_{\theta_4=0}\right) - \frac{\pi}{2} \tag{19} $$

3.6. Joint 6

Because the *x*-axis of frame 6 is parallel to that of frame 5 when $\theta_6 = 0$ and θ_6 is the angle from the *x*-axis of frame 5 to that of frame 6, θ_6 is equal to the angle from *x*-axis of frame 6 at $\theta_6 = 0$ to the current *x*-axis of frame 6 as shown in Fig.7. Let $\theta_6 = 0$, we have transformation matrix

$$ {}_6^0T\Big|_{\theta_6=0} = \begin{bmatrix} {}_6^0R'_{11} & {}_6^0R'_{12} & {}_6^0R'_{13} & {}_6^0P_{ORGx} \\ {}_6^0R'_{21} & {}_6^0R'_{22} & {}_6^0R'_{23} & {}_6^0P_{ORGy} \\ {}_6^0R'_{31} & {}_6^0R'_{32} & {}_6^0R'_{33} & {}_6^0P_{ORGz} \\ 0 & 0 & 0 & 1 \end{bmatrix} \tag{20} $$

The unit vectors of frame 6 when $\theta_6 = 0$ are

$$ \overrightarrow{{}_6^0X_6}\Big|_{\theta_6=0} = \begin{bmatrix} {}_6^0R'_{11} \\ {}_6^0R'_{21} \\ {}_6^0R'_{31} \end{bmatrix}, \ \overrightarrow{{}_6^0Y_6}\Big|_{\theta_6=0} = \begin{bmatrix} {}_6^0R'_{12} \\ {}_6^0R'_{22} \\ {}_6^0R'_{32} \end{bmatrix} \tag{21} $$

From equation (1), the x-axis unit vector of frame 6 when $\theta_6 \neq 0$ is

$$ \overrightarrow{{}_6^0X_6} = \begin{bmatrix} {}_6^0R_{11} \\ {}_6^0R_{21} \\ {}_6^0R_{31} \end{bmatrix} \tag{22} $$

The joint angle of joint 6 can be calculated as follows

$$ \theta_6 = Atan2\left(\overrightarrow{{}_6^0X_6} \cdot \overrightarrow{{}_6^0Y_6}\Big|_{\theta_6=0}, \overrightarrow{{}_6^0X_6} \cdot \overrightarrow{{}_6^0X_6}\Big|_{\theta_6=0}\right) \tag{23} $$

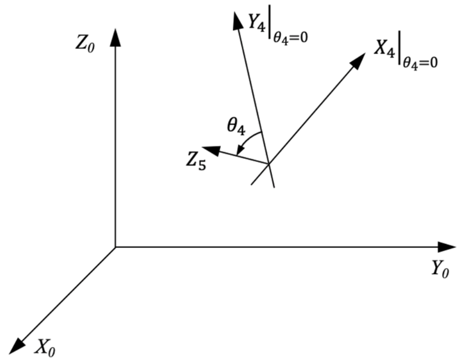

Fig.6 Joint angle calculation of joint 4

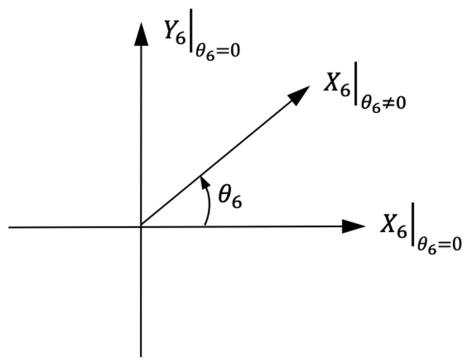

Fig.7 Joint angle calculation of joint 6

4. Experimental verification

In order to verify the proposed geometric approach for inverse kinematics of the robot arm, implementation of the joint angles is conducted and the results are compared with exact values. The test is achieved by the following steps:

(1) Choose a series of joint angles randomly and do forward kinematics calculation to get the position and orientation of the robot arm effector.

(2) Calculate the joint angles by using the inverse kinematics solution. Since there are multiple solutions, choose the ones

(3) Compare the joint angles obtained from step (1) and (2) to get the largest error.

(4) Run the above steps 50 times.

Fig.7 shows the calculated errors of joint angles in degree. As it can be seen, the error for most runs is zero, except for those joint angles approaching zero. The results indicate that the proposed geometric solution for inverse kinematics is correct and accurate.

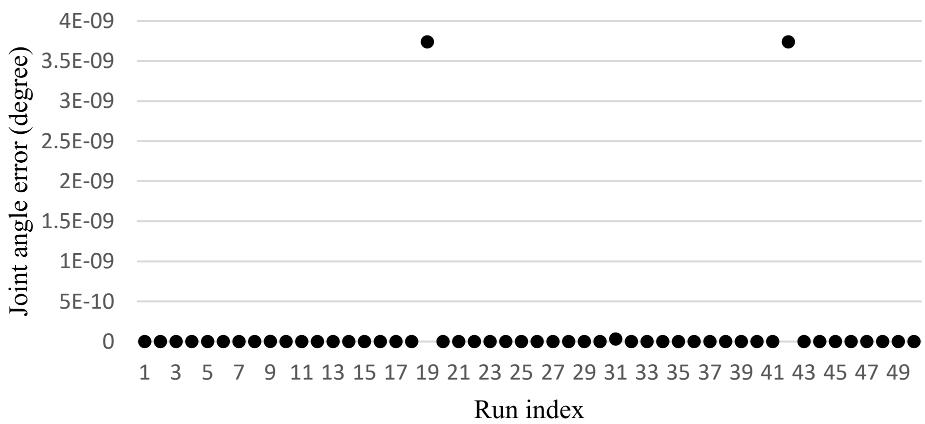

Fig.8 Joint angle error

5. Conclusion

Based on the derivation and experimental verification presented above, some conclusions can be drawn as below:

(1) For an articulated 6-ODF robot arm which has three neighboring joint axes intersecting at a point, there exist geometric solutions for each joint angle.

(2) The proposed geometric solutions for inverse kinematics are verified to be accurate.

(3) The proposed geometric approach is easy to understand and at low computational cost.

Acknowledgments
This work is financially supported in part by the Natural Science Foundation of Inner Mongolia (2020MS01012) and Science and Technology Planning Project of Guangxi Zhuang Autonomous Region (AD21220141).

References
[1] Craig, J. J. (2004) Introduction to Robotics: Mechanics and Manipulations, 3rd ed. Pearson Education.
[2] Lynch, K. M., Park, F. C. (2017) Modern Robotics: Mechanics, Planning, and Control, Cambridge University Press.
[3] Kalajahi, E. G., Mahboukkhah, M. (2021) Numerical Versus Analytical Direct Kinematics in a Novel 4-DOF Parallel Robot Designed for Digital Metrology. IFAC-PapersOnLine, 154(1): 181-186.
[4] Sekiguchi, M, Takesue, N. (2021) Numerical method for inverse kinematics using an extended angle-axis vector to avoid deadlock caused by joint limits. Advanced Robotics, 135(15):919-926.
[5] Takesue, N, Sekiguchi, M. (2019) Cooperative and robotized system and expansion of kinematics. J Rob Soc Jpn. 37(10):919–922.
[6] Hemami, A, Labonville, R. (1988) Kinematic equations and solutions of a human-arm-like robot manipulator. Robotics and Autonomous Systems, 4(1): 65-72.
[7] Wang, K., Lien, T. K. (1988) Structure design and kinematics of a robot manipulator. Robotica, 6(4): 299-309.
[8] Lloyd, J., Hayward, V. (1988) Kinematics of common industrial robots. 4(2):169-191.
[9] Tsai, L. W., Morgan, A. P. (1985) Solving the Kinematics of the Most General Six- and Five-Degree-of-Freedom Manipulators by Continuation Methods. Journal of Mechanisms, Transmissions, and Automation in Design, 107:189-200.
[10] Khatamian, A. (2015) Solving Kinematics Problems of a 6-DOF Robot Manipulator. Int'l Conf. Scientific Computing, 228-233.
[11] Tian, X., Xu, Q., Zhan Q. (2021) An analytical inverse kinematics solution with joint limits avoidance of 7-DOF anthropomorphic manipulators without offset. J Franklin Inst., 358(2):1252–1272.
[12] Yu, C., Jin, M., Liu, H. (2012) An analytical solution for inverse kinematic of 7-DOF redundant manipulators with offset-wrist. IEEE Int Conf Mechatron Autom, 92–97.
[13] Almusawi, A, Dulger, L. C., Kapucu. S. (2016) A New Artificial Neural Network Approach in Solving Inverse Kinematics of Robotic Arm (Denso VP6242). Computational Intelligence and Neuroscience, 2016: 1-10.
[14] Toquica, J. S., Oliveira, P. S., Souza, W. S. R, et al. (2021) An analytical and a Deep Learning model for solving the inverse kinematic problem of an industrial parallel robot. Computers & Industrial Engineering, 151: 106682.
[15] Jiokou, G., Melingui, A., Lakhal, O. et al. (2020) A Learning Framework to Inverse Kinematics of Redundant Manipulators. IFAC-PapersOnLine, 53(2): 9912-9917.